Effect of atmospheric aerosol on surface ozone variation over the Pearl River Delta region

DENG XueJiao[1*], ZHOU XiuJi[2], WU Dui[1], TIE XueXi[3], TAN HaoBo[1], LI Fei[1], BI XueYan[1], DENG Tao[1] & JIANG DeHai[1]

[1] Institute of Tropical and Marine Meteorology/ Key Open Laboratory for Tropical Monsoon, China Meteorological Administration, Guangzhou 510080, China;
[2] Chinese Academy of Meteorological Sciences, CMA, Beijing 100081, China;
[3] National Center for Atmospheric Research, Boulder, CO, USA

Our analysis of the surface aerosol and ultraviolet (UV) measurements in Pearl River Delta (PRD) region shows that the surface UV radiation is reduced by more than 50% due to high aerosol concentrations. This has important impacts on urban ecosystem and photochemistry, especially on ozone photochemical production over the region. The quantitative effect of aerosols on surface ozone is evaluated by analyzing surface observations (including ozone, ultraviolet radiation, aerosol radiative parameters) and by using radiative and chemical models. A case study shows that the aerosol concentrations and UV radiation are significantly correlated with ozone concentrations. The correlation coefficient between the aerosol optical depth (AOD) and the PM_{10} mass concentration is very high, with a maximum of 0.98, and the AOD and UV radiation/ozone is anti-correlated, with a correlation coefficient of −0.90. The analysis suggests that ozone productivity is significantly decreased due to the reduction of UV radiation. The noon-time ozone maximum is considerably depressed when AOD is 0.6, and is further decreased when AOD is up to 1.2 due to the reduction of ozone photochemical productivity. Because the occurring probability of aerosol optical depth for $AOD_{550nm} \geqslant 0.6$ and $AOD_{340nm} \geqslant 1.0$ is 47, and 55% respectively during the dry season (October, November, December, January), this heavy aerosol condition explains the low ozone maximum that often occurs in the dry season over the Guangzhou region. The analysis also suggests that the value of single scattering albedo (SSA) is very sensitive to the aerosol radiative effect when the radiative and chemical models are applied, implying that the value of SSA needs to be carefully studied when the models are used in calculating ozone production.

atmospheric aerosol, ozone, photochemical process, attenuation

The concept of MAP (Metro-Agro-Plexes) was proposed by Chameides et al. [1], in which they also discussed the possible influences of photochemical pollution caused by regional industrial urban and rural emission on global ecosystem. Dickerson et al. [2] estimated the effects of aerosols on ultraviolet radiation and photochemical oxidants, showing that absorptive aerosols resulted in O_3 decreasing by 24 ppbv. Meinrat and Crutzen [3] and Lack et al. [4] discussed the bio-geo-chemical sources of atmospheric aerosols and their roles in the atmospheric chemistry. Tie and Cao [5] and Deng et al. [6] showed that aerosols have an important impact on ozone production over China. Those studies showed the important interaction between aerosol and photochemistry (O_3). In polluted urban atmosphere, the rate of

*Corresponding author (email: dxj@grmc.gov.cn)

photochemical O_3 production is not only related to the ozone precursors NOx and VOCs but also closely depended upon the UV flux, which is the driving force for the O_3 photochemistry [7] Ozone photochemistry is a very complicated process and under NO_x-limited condition, ozone productivity is determined by NOx concentrations and the intensity of UV radiation; while under VOCs-limited condition, ozone productivity is determined by VOCs concentrations and the intensity of UV radiation. In the past, the interaction between O_3 and its precursors (NO_x and VOCs) was intensively studied in China [8–22]. However, less attention was paid to the interaction between UV radiation and other important photochemical factors (including radicals, photochemical rates, and atmospheric oxidation ability), which affect the ozone photochemical formation. Because the photochemical characteristics of pollutants are different in different regions, the O_3 photochemical production is strongly varied in different regions, which were shown by the many studies [23–29].

An international regional experiment project for the study of tropospheric aerosols over Eastern Asia was conducted by Sino-USA scientists in 2004 [30]. The characterizations of aerosols and their effects on solar shortwave radiations and ultraviolet radiation were analyzed. The result suggested that aerosols strongly reduced the solar radiation in the northern region of China [31–33]. The study in recent years also showed that under current pollution condition in the Pearl River Delta (PRD) region, more than half of surface UV radiation has been reduced by aerosols [34], inducing important influence on the O_3 photochemical processes over the region. Thus, it is necessary to study the individual effects of the aerosols and the changes in ozone precursors on ozone photochemistry in the PRD region. The measured ozone concentrations in the PRD region show that the ozone episodes with high concentrations (hourly maximum O_3 >120ppb) often occur in spring, summer, and autumn. Because the aerosol concentrations are considerably higher in autumn than in other seasons in the PRD region, we select the data in autumn season as a case study to estimate the interaction between aerosol pollution and ozone photochemical process.

1 Data and NCAR TUV radiative and MM chemical models

Since 2004, Guangdong Provincial Meteorological Bureau (GMB) has established a measurement network of atmospheric composition. The main station is located in Dazhenggang Mountain, Nancun County in Guangzhou's Fanyu district (station ID:59481). Fanyu is an administration district of Guangzhou, and is located in southern part of Guangzhou city, the center of the PRD region. The Dazhenggang Mountain is the summit of Fanyu district, with altitude of 141m. The longitude and latitude are 113°21′E,

23°00′N respectively. A sub-station is located in Fanyu Meteorological Bureau with altitude, longitude, and latitude being 13 m, 113°19′E, and 22°56′N respectively. The distance between the main and sub-stations in Fanyu district is 8 Km, and the altitude difference between the main station and sub-stations is 128m. The data used in this study were collected at the main station from November 2005 to May 2007 and at the sub-station from April 2006 to May 2007. The UV radiation data are from Eppley TUVR meter observation. The aerosol size distribution is observed by Grimm Model 180 instrument. The aerosol optical depth (AOD) is observed by portable sunphotometer Microtops II Sunphotometer. The detail description of the above instruments was given by Wu et al. [35].

The radiative transport model used in the paper is the NCAR Tropospheric Ultraviolet and Visible Radiation Model (TUV), which was developed by Madronich and Flocke [36] at National Center of Atmospheric Research (NCAR), The TUV Model calculates tropospheric UV and visible radiation, with wave spectrum from 121 to 735 nm. The TUV model calculates not only the UV irradiance but also the actinic flux and the molecule photodissalation rate. The 4-stream scheme is used to solve the radiative transport equation in the model.

The NCAR Master Mechanism Box Chemical Model (MM) was developed by Madronich and Calvert [37] at National Center of Atmospheric Research (NCAR) in 1989, and there were several improvements afterwards. The NCAR-MM model is a chemical model that includes a detailed and flexible chemical scheme [38]. The model is a box (0-D) model with detailed gas phase chemistry, including 5000 reactions and 2000 chemical species. This model computes the time-dependent chemical evolution with a prescribed initial condition. This model is useful to study complex chemical processes with regional emissions. Thus, the box model provides an opportunity to examine chemical transformations of an isolated urban plume at a level of detail that would be impractical to implement in current 3D models. The hydrocarbon chemistry in the master mechanism is treated explicitly and includes the photo-oxidation of partly oxygenated organic species. Alkanes, alkenes and aromatics are considered as initial hydrocarbon reagents in the gas-phase mechanism. The chemistry of the methyl peroxy radical is treated explicitly; a counter scheme is used for the other organic peroxy radicals. The rate coefficients for organic peroxy radical reactions were updated based on recent recommendations by Tyndall et al. [39]. Rate coefficients for hydrocarbons reactions with OH were updated based on the latest JPL compilations by DeMore et al. [40]. The OH-initiated ethene oxidation mechanism was modified to include multiple branchings for the β-hydroxyl ethoxy radical reaction with NO [41]. OH-initiated rate coefficients for oxygenated hydrocarbons were updated from the Atkinson et al. [42] compilation. The kinetics of the HO_2 self-reaction were recently measured by Christensen et al.

[43] to be lower than the current recommendation. The photolysis rate (J value) is calculated on-line with NCAR MM using radiative transfer code (TUV). The TUV module was initialized for the various cases with measured median values for latitude, Julian day, altitude, O_3 column, and albedo. The TUV module was updated with cross section and quantum yields from recent evaluations for inorganic species by DeMore [40] and organic species by Atkinson et al. [42]. NCAR-MM has 73 photochemical reactions. OH is formed by the H_2O reacted with O from O_3 photodecomposition in the troposphere, which is the original source of OH in the tropospheric atmosphere; the OH controls the main chemical reactive processes of the major mass in the troposphere. O_3 is formed by the oxidation of OH with CO and HC (hydrocarbon); the O_3 diurnal pattern is similar to that of OH, which is controlled by photochemical reaction. Based on the ozone photochemical theory, the O_3 productivity is closely related with the UV radiation [44], and ultraviolet radiation (100–400nm) plays an important role in the OH and O_3 forming processes, the specific spectrum dissa specific mass. For example, the spectrum between 202 and 422 is the important photolysis wavelength for the ozone forming, so the factor that influences the UV radiation will simultaneously affect the O_3 productivity.

2   The characterizations of measured surface ozone

Figure 1 shows the monthly mean ozone concentrations at the main station and the Fanyu sub-station. The result shows that the monthly and seasonal variations are very similar at the two stations. Several high ozone peaks are indicated in Figure 1, including in spring (April at the main station and May at the sub-station), in summer (August), and in autumn (October). Several ozone minima are also shown in Figure 1, occurring in winter (December, January, February), early spring (March), and the early summer (June), with lowest concentrations in December, January, February, and March. According to Wang et al. [45], the ozone concentrations measured from several stations in the Hong Kong region

had an ozone peak in autumn, and an ozone minimum in summer. The above ozone features are very different compared to the observations in mid-latitude regions (e.g., North America, Europe, Yangtze delta, Beijing) [46, 47], where ozone peaks are often observed in spring and summer (May and June). This unique ozone seasonal variation in PRD region is closely related to large-scale atmospheric circulation (Asian monsoon). In the summer monsoon period, marine cleaner air mass results in an ozone minimum at large area over the PRD region in June and July, whereas in the winter monsoon period, the local pollution and the polluted air mass from upstream continents produce a high ozone concentration over PRD region [48–50]. The ozone diurnal variations at the main and sub-stations show that ozone has a solo-peak with the maxima occurring in afternoon (14:00, 15:00, and 16:00). In general, the solar radiation peak occurs at the noon (12:00), and ozone diurnal peak often occurs about 2–4 hours later than the solar radiation peak, which is the common ozone diurnal pattern in many places. Based on the analysis of the ozone concentration probability at the two stations, the probability of ozone less than 50ppb and larger than 80ppb of Guangzhou main station are 91, 4%, respectively. Table 1 shows the details of the statistics of ozone concentrations at Guangzhou main station (November 2005–May 2007) and Fanyu sub-station (April 2006–May 2007). Table 1 also shows the maximum ozone seasons are spring and summer (from April to August), while there are few times that ozone concentrations were greater than 120 ppb, which occurred in autumn and winter (except September 2006). Although the mean ozone in June is the lowest, the high ozone concentrations (larger than 120 ppbv) occur on 11, 22, 27 June 2006 at Fanyu sub-station. These high ozone concentrations occurred mostly in April at Guangzhou main station. Although the mean ozone is higher in October, no high ozone concentrations (greater than 120 ppb) occurred. The above high ozone-occurring seasons are consistent with the values of the middle latitude regions (North America, Europe, Yangtze River Delta, Beijing) [46, 47], where measured high ozone concentrations often occurred in Spring and Summer. The above analysis shows that the seasonal features of mean
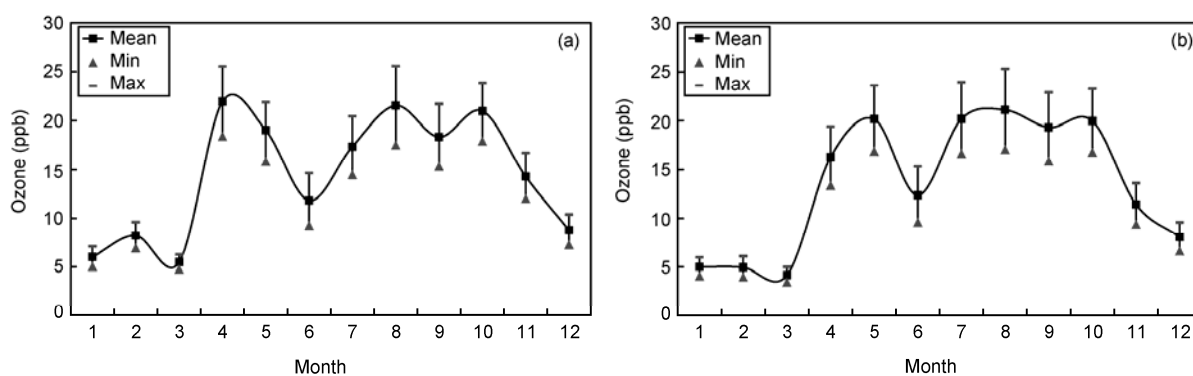

Figure 1   The ozone monthly variation at Guangzhou main station (a) and Fanyu sub-station (b).

Table 1 The occurring date, occasions, extremum and time of ozone maximum ≥120 ppb at main station

Date	Number	Mean	Min	Max	Time_max
Guanzhou main station [a]					
2006-04	3	123	90	140	2006-04-20 15:05
2006-05	2	123	97	133	2006-05-11 13:40
2006-07	2	121	113	125	2006-07-24 14:00
2006-08	3	125	118	134	2006-08-13 17:15
2007-04	20	130	51	218	2007-04-26 18:00
Fanyu sub-station [b]					
2006-04	3	130	71	156	2006-04-20 14:25
2006-05	8	115	53	155	2006-05-11 15:05
2006-06	8	115	58	149	2006-06-11 15:30
2006-07	14	120	80	146	2006-07-24 12:40
2006-08	21	119	83	158	2006-08-13 16:35
2006-09	1	110	93	122	2006-09-26 17:25
2007-04	3	124	108	133	2007-04-26 16:55

a) Data cover November 2005–May 2007, data time resolution is 5 min; b) data cover April 2006–May 2007, data time resolution is 5 min

ozone are different from that of the maximum ozone in the PRD region.

3 Effect of atmospheric aerosol on surface ozone

3.1 Effect of aerosol on surface ultraviolet radiation and ozone by observational analysis

Figure 2 shows the variations of aerosol optical depth (AOD at 550 nm) and surface aerosol mass PM_{10} concentrations on 17–27 December 2006. Figure 3 shows the variations of surface UV (12:00) and O_3(12:00–14:00) on 17–27 December 2006. We can see that the AOD on date 20, 24, 26 December 2006 is larger than the value of the day before, which corresponds to the relative lower UV and O_3 values. This result suggests that heavier aerosol results in lower UV, producing lower O_3 concentrations. This is a good example to study the effect of aerosol on UV radiation and O_3 chemical production. Table 2 shows the correlation coefficients among several physical parameters on 17–27 December 2006. The result shows that the correlation coefficient between AOD and PM_{10} reaches 0.98, indicating that the variation of surface aerosol concentration is consistent with AOD variation. The correlations between AOD and UV, O_3 at 12:00 are anti-correlated with a correlation coefficient of −0.9. The relationship between AOD (12:00) and O_3 (13:00, 14:00) also shows anti-correlation. The correlation coefficient between AOD at 12:00 and O_3 at 13:00 is −0.91, and the correlation coefficient between AOD at 12:00 and O_3 at 14:00 is weaker (−0.76). The high anti-correlation between AOD (12:00) and O_3 (13:00, 14:00) indicates the influence of aerosol particles on O_3 concentrations is strong with 1–2 hour time lag. The relationship between UV and O_3 is a positive correlation, and the relationship between UV at 12:00 and O_3 at 13:00 is almost the

same as that relationship between UV at 12:00 and O_3 at 12:00, and weaker with O_3 at 14:00.

The analysis shows that the pollutions are heavier on 20, 24, 26 December 2006 than the day before, and we label the dates of 20, 24, and 26 as the pollution condition, but the dates of 19, 23, and 25 as the clean condition. Figure 4 shows the comparisons of aerosol surface area, aerosol optical depth, ultraviolet radiation, O_3, O_3 maximum occurring time and O_3 productivity under clean and pollution conditions. The figure shows that under the clean condition, the aerosol surface area with diameters of 0.25–1.0, 1.0–2.5, and 2.5–10.0 μm are 153, 8, 17 $μm^2/cm^3$ respectively. The average AOD at 550nm is 0.28; the UV (315–400 nm) at 12:00 is 45 W/m^2; and O_3 at 12:00, 13:00, 14:00 and daily O_3 maximum are 21.8, 24.6, 25.3, 27.4 ppb respectively. The O_3 maximum occurring time is at 14:45PM, and the O_3 productivity $d[O_3(12:00–9:00)]/dt$ is 5.0 ppb/hour. While under the pollution condition, the aerosol surface area with diameters of 0.25–1.0, 1.0–2.5, 2.5–10.0 μm are 271, 15, 32 $μm^2/cm^3$, respectively, and the average AOD at 550nm is 0.62; the UV (315–400 nm) at 12:00 is 37 W/m^2; and O_3 at 12:00, 13:00, 14:00 and daily O_3 maximum are 13.4, 15.7, 18.9, 24.4 ppb respectively. The O_3 maximum occurring time is at 15:52 PM, and the O_3 productivity $d[O_3(12:00–9:00)]/dt$ is 3.5 ppb/hour.

The above analysis shows that under the clean condition, aerosol surface area and the optical depth are smaller, while UV, O_3 and O_3 productivity are larger, and the occurring time of daily O_3 maximum is earlier. The surface area of aerosol with diameter less than 1 μm contains most of the surface area (above 85%) under both the clean and pollution conditions. The portion is almost the same under the clean and pollution conditions. Based on mie-scattering theory, the scattering efficiency of aerosol with diameter less than 1 μm is larger. As a result, under the pollution condition, fine aerosol particles play important roles in resulting in the reduction of UV radiation and lower O_3 productivity.
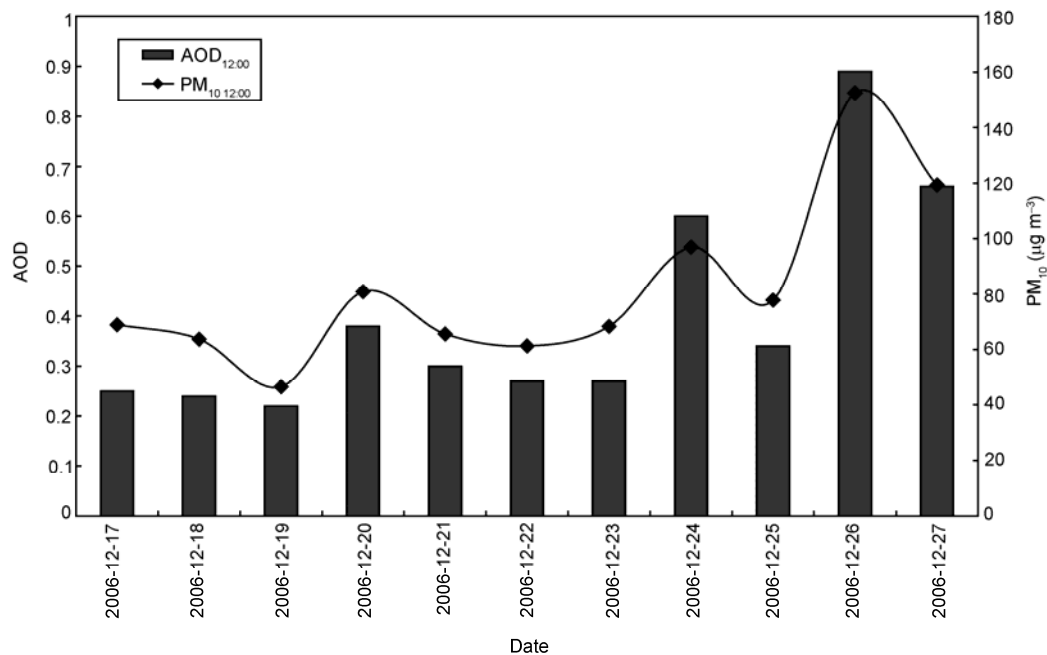
Figure 2   The variations of 550nm AOD and surface PM_{10} on 17–27 December 2006.
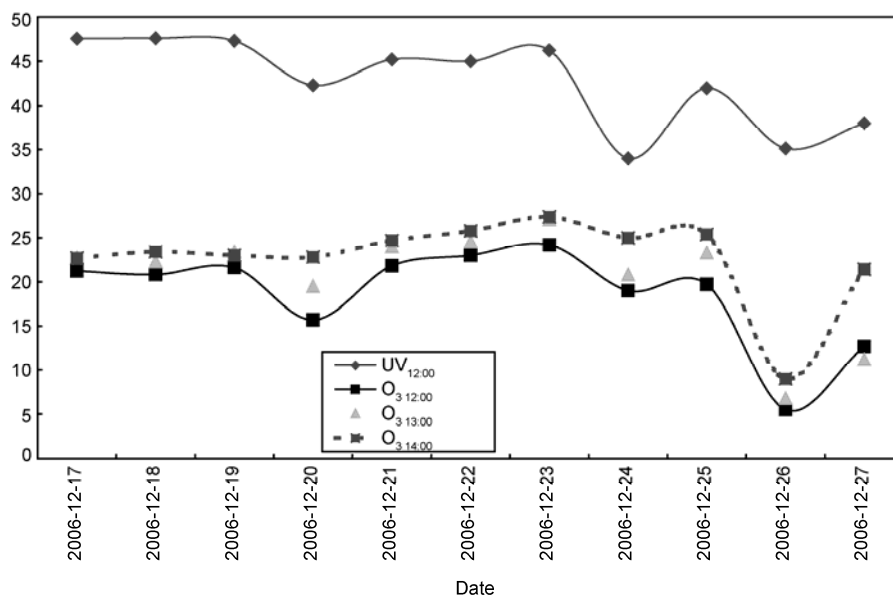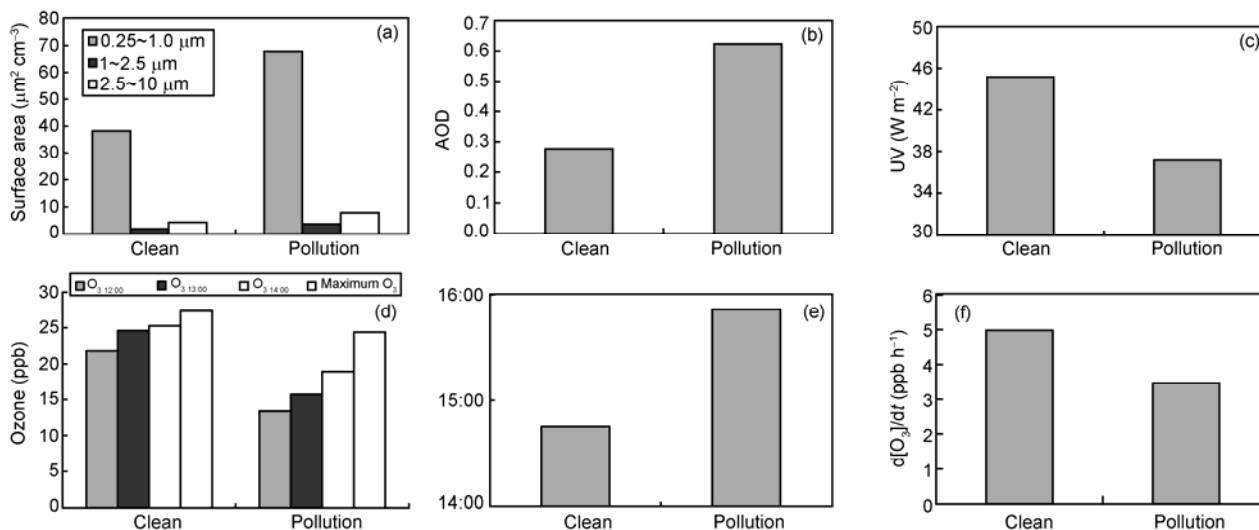

Figure 3   The variations of surface UV (12:00) and O_3 (12:00–14:00) on 17–27 December 2006.

Table 2   The correlation coefficients among several physical parameters on 17–27 December 2006

| Correlation coefficient	$AOD_{12:00}$	$PM10_{12:00}$	$UV_{12:00}$	$O3_{12:00}$	$O3_{13:00}$	$O3_{14:00}$
$AOD_{12:00}$	1					
$PM_{10\ 12:00}$	0.98	1				
$UV_{12:00}$	−0.92	−0.85	1			
$O_{3\ 12:00}$	−0.91	−0.93	0.73	1		
$O_{3\ 13:00}$	−0.91	−0.93	0.72	0.98	1	
$O_{3\ 14:00}$	−0.76	−0.79	0.50	0.90	0.88	1

Figure 4   The comparisons of aerosol surface area (12:00, (a)), aerosol optical depth (12:00, (b)), ultraviolet radiation (12:00, (c)), O_3 (d), O_3 maximum occurring time (e) and O_3 productivity (f) under clean and pollution condition. The clean condition is the mean of date 19, 23, 25; the pollution condition is the mean of date 20, 24, 26.

3.2   The attenuation of atmospheric aerosols on surface ozone by model analysis

In the period of 17–27 December 2006, the AOD is 0.3 and 0.6, respectively under the clean and pollution conditions. The wavelength exponent is about 1.4. The average aerosol single scattering albedo (SSA) of the whole column atmosphere of the process is about 0.9 [34] in the PRD region. Based on the above aerosol optical property parameters, the reasonable actinic radiation flux can be calculated. Figure 5 shows the measured and calculated (by the NCAR-MM model) ozone diurnal variations under the pollution and clean conditions. It shows that the measured ozone concentrations under the clean condition (AOD=0.3) are larger than that of the pollution condition (AOD=0.6). The ozone concentrations simulated by the model also show the effects of AOD on ozone concentrations, e.g., lower ozone concentrations under the higher AOD condition. Because the model calculation just changes the AOD value under the pollution condition, while the concentrations of ozone precursors and other factors kept unchanged, the model calculation suggests that the lower ozone concentrations are only due to the higher aerosol condition. The largest difference of ozone diurnal variation under different AOD conditions occurs at 15:00–16:00, which is the time when ozone maximum often appears. This feature indicates that the existence of aerosol particles has a significant influence on ozone peak occurring time and the magnitude of ozone concentration. When the values of AOD are 0.0, 0.3, 0.6, and 1.2, respectively, the model-calculated ozone maximum is 32, 25, 21, and 15 ppb respectively. The ozone reductions are 16% and 28%, when AOD increase from 0.3 to 0.6 and from 0.6 to 1.2, respectively, indicating that the reduction of ozone due to aerosol is larger with the increase of aerosol

concentrations. The ozone peak disappears when AOD is 0.6, and the ozone peak turns to a decreasing trend when AOD is larger than 1.2. In the dry season (Oct, Nov, Dec, and Jan) the occurring probability of aerosol optical depth for $AOD_{550\,nm} \geqslant 0.6$ and $AOD_{340\,nm} \geqslant 1.0$ is 47%, and 55%, respectively, suggesting that the heavy aerosol in Guangzhou has important impacts on ozone concentrations and ozone diurnal variations during the dry season. The above study is helpful for better understanding the ozone control strategy and the productive efficiency of ozone peak [51].

Figure 6 shows the measured and simulated O_3 variation during the period of 17–27 December 2006. The observed ozone reduction under the pollution condition (AOD=0.6) is 60% compared to the clean condition (AOD=0.3) in morning, decreasing to 30% at noon, and increasing to 60% in the evening. This result indicates that the effect of aerosol on ozone variation is more significant in morning and evening. The NCAR-MM model calculation is similar to the measured result, with 25% reduction in morning, decreasing to 15% at noon, and increasing to 25% in evening. However, the calculated ozone reduction is generally smaller than the measured ozone reduction. The reason for the calculated smaller ozone reduction is that the simulated ozone reduction by the NCAR-MM model takes into account only the effect of aerosol on actinic radiation, while the measured result includes other factors (such as multiphase chemistry, the variation of ozone precursors etc. Marked as Other influence factors=Observation$_{(Pollution\ compared\ to\ Clean)}$−MM$_{(Pollution\ compared\ to\ Clean)}$ in Figure 6). The effect of other factors inhibits the ozone forming in morning, and the inhibition is smaller till noon, but the inhibition turns to the positive effect at 15:00–16:00 (the red circle in Figure 6) which accelerates the ozone forming. Figure 6 also shows that the ozone reduction under the pollution condition (AOD=0.6)
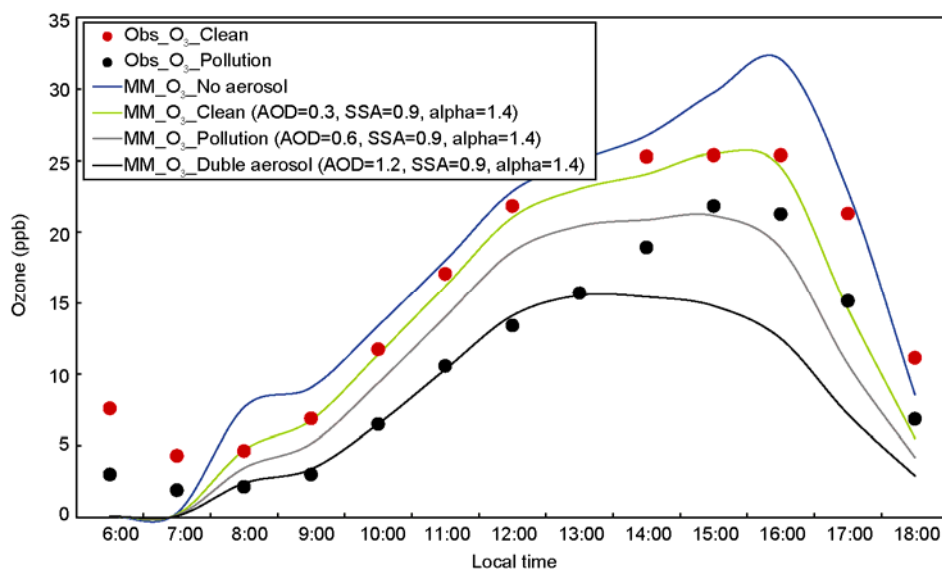
Figure 5   The observed and simulated O_3 diurnal variation under pollution and clean condition on 17–27 December 2006.
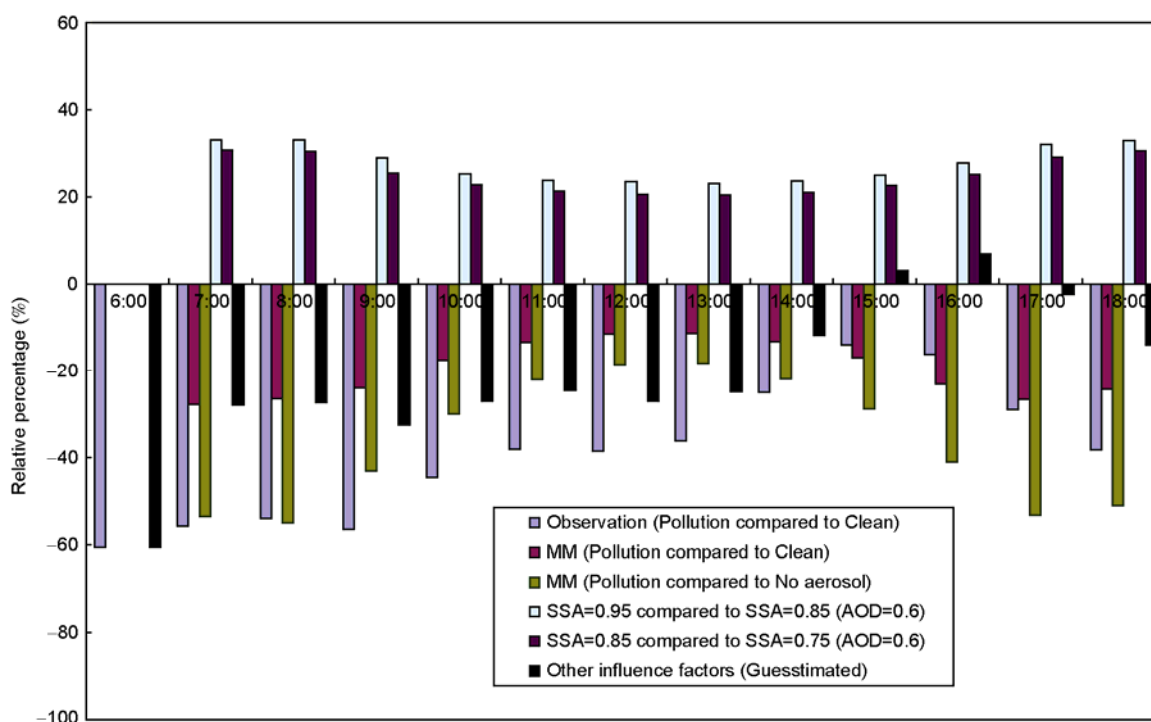
Figure 6   The observed and simulated O_3 diurnal variation range on 17–27 December 2006.

compared to no aerosol (AOD=0.0) is 1.6–2.1 times larger than that under the pollution condition (AOD=0.6) compared to clean condition (AOD=0.3), indicating the double increase of AOD would result in double increase of ozone reduction in morning and in evening, and about 1.6 times at noon. In addition, the increase in SSA by 0.1 results in ozone increase by more than 23%, with a larger increase in ozone when the values of SSA are larger. The ozone increase rate is larger in morning and evening than at noon,

and the diurnal increase rate is about 10%.

The above analysis shows that aerosol particles result in the lower ozone productivity through the reduction of ultra-violet radiation. The effect of aerosol on ozone is −28% in the pollution condition during the period of 17–27 December 2006, producing lower ozone peak in the afternoon. The increase in SSA by 0.1 would result in ozone increase by more than 33%. Therefore, it is important to select the SSA value in the model calculation. For example, if the selected

SSA value is 0.1 smaller than real value, it could induce about 33% error in ozone calculation, which is impossible to accurately calculate the impact of aerosol on ozone concentrations

4   Conclusions

(1) In the PRD region, the seasonal features of mean ozone are different from that of the maximum ozone. The high mean ozone occurs in spring (April, May), summer (August), and autumn (October). The low ozone occurs in winter (December, January, and February), early spring (March), and summer (June). The minimum ozone occurs in December, January, February, and March. The minimum ozone in summer and autumn occurs in June. The maximum ozone (>120 ppb) occurs in spring and summer (April, May, June, July, and August). The mean ozone in June is relatively lower, but the high ozone episode (ozone>120 ppbv) often occurs. The mean ozone in October is relatively high, but no maximum ozone (>120 ppb) episode was observed.

(2) The case analysis shows that there a close correlation among aerosol, ultraviolet radiation, and ozone. The correlation coefficient between AOD and surface PM_{10} concentration is very high (0.98), while the anti-correlation between AOD and UV, O_3 also high, with correlation coefficient of -0.90.

(3) The aerosol particles reduce ozone productivity through the decrease in ultraviolet radiation, reducing the occurrence of ozone peak in afternoon. The reduction of aerosol particles on ozone is more evident with the enhancement of AOD. Under current ozone precursor condition, the ozone's largest reduction rates are 16% and 28%, when the values of AOD increase from 0.3 to 0.6 and from 0.6 to 1.2, respectively. The ozone peak disappears when the value of AOD reaches 0.6, and the ozone peak turns to a decreasing trend when the value of AOD is larger than 1.2. This result shows clear evidence that aerosol particles result in lower ozone productivity, and reduce the occurrence of ozone maximum in the afternoon. At present, the probability of aerosol optical depth with $AOD_{550\,nm}>0.6$ and $AOD_{340\,nm}>1.0$ is 47% and 55% in the dry season, respectively. As a result, this heavy aerosol pollution in Guangzhou produces important effect on ozone photochemical production in the dry season.

(4) By using radiative model, we can calculate the different rates of reduction of surface radiation with the different values of AOD. However, the selection of SSA values has a large impact on the calculated result. Thus, the values of SSA must be carefully studied and selected.

1   Chameides W L, Kasibhatl P S, Yienger J, et al. Growth of continental-scale Metro-Agro-Plexes, regional ozone pollution and world food production. Science, 1994, 264: 74–77

2   Dickerson R R, Kondragunta S, Stenchikov G, et al. The impact of aerosols on solar ultraviolet radiation and photochemical smog. Science, 1997, 278: 827–830

3   Meinrat O A, Crutzen P J. Atmospheric aerosols: biogeochemical sources and role in atmospheric chemistry. Science, 1997, 276: 1052–1058

4   Lack D, Tie X, Neville A, et al. Seasonal variability of atmospheric oxidants due to the formation of secondary organic aerosol: A global modeling study. J Geophys Res, 2003, 108, doi: 10.1029/2003JD003418

5   Tie X, Cao J. Aerosol pollutions in eastern China: Present and future impacts on environment. Particuology, 2009, 7: 426–431

6   Deng X J, Tie X, Zhou X J, et al. Effects of biomass burning in southeast Asia on aerosol and ozone concentrations over Pearl River Delta (PRD) region. Atmos Environ, 2008, 42: 8493–8501

7   Tie X, Madronich S, Walters S, Rasch P, et al. Effect of clouds on photolysis and oxidants in the troposphere. J Geophys Res, 2003, 108: 4642, doi: 10.1029/2003JD003659

8   Tang X Y. Atmospheric Environmental Chemistry (in Chinese). Beijing: Higher Education Press, 1990

9   Zhou X J. The Atmospheric Ozone Variation and Its Effect on Climatic Environment over China (1) (in Chinese). Bejing: Meteorology Press, 1996

10 Wang M X. Atmospheric Chemistry. Second Edition (in Chinese). Beijing: Meteorology Press, 1999

11 Zhang Y H, Shao K S, Tang X Y. The study of urban photochemical smog pollution in China. Acta Sci Nat Univ Pekinensis, 1998, 34: 392–400

12 Ji F, Su W Y, Qin Y. A study of the gas-to-particle conversion in photochemical process. Chin J Atmos Sci, 2001, 25: 269–276

13 An J L,Gao H W,Wang Z F, et al. Effects of changes in the concentration of nonmethane hydrocarbon (NMHC) at high NOx content on amount of ozone formation. Clim Environ Res,1998, 3: 147–150

14 An J L, Hang Z W, Wang Z F, et al. Impacts of changes in the concentration of nonmethane hydrocarbon (NMHC) and NOx on amount of ozone formation. Chin J Atmos Sci, 1999, 23: 753–761

15 An J L.Ozone production efficiency in Beijing area with high NOx emissions. Acta Sci Circumstantiae, 2006, 26: 652–657

16 Liu J F, Li J L, Bai Y H. A comparison of atmospheric photochemical mechanisms (I) O_3 and NO_x. Environ Chem, 2001, 20: 305–312

17 Liu J F, Li J L, Bai Y H. A comparison of atmospheric photochemical mechanisms (II) HO_x and photochemical oxides. Environ Chem, 2001, 20: 313–319

18 Wang X S, Li J L. The contribution of anthropogenic hydrocarbons to ozone formation in Beijing areas. China Environ Sci, 2002, 22: 501–505

19 Zhu B, Li Z H,Xiao H,et al. Simulation research of photochemical ozone creation potential of NMHC. J Nanjing Inst Meteorol, 2000, 23: 228–345

20 Tie X, Brasseur G, Zhao C, et al. Chemical characterization of air pollution in eastern China and the eastern United States. Atmos Environ, 2006, 40, 2607–2625

21 Tie X, Chandra S, Ziemke J R, et al. Satellite Measurements of tropospheric column O_3 and NO_2 in eastern and southeastern Asia: Comparison with a global model (MOZART-2). J Atmos Chem, 2007, 56: 105–125, doi: 10.1007/s10874-006-9045-7

22 Tang W Y, Zhao C S, Geng F H, et al. Study of ozone "weekend effect" in Shanghai Sci China Series D-Earth Sci, 2008, 51: 1354–1360

23 Tie X, Guenther A, Holland E. Biogenic methanol and its impact on tropospheric oxidants. Geophys Res Lett, 2003, 30, 1881, doi: 10,1029/2003GL017167

24 Tie X, Madronich S, Stacy W, et al. Assessment of the global impact of aerosols on tropospheric oxidants. J Geophys Res, 2005, 110: D03204, doi: 10.1029/2004JD005359

25 Zhang R, Lei W, Tie X, Hess P. Industrial emissions cause extreme diurnal urban ozone variability. Proc Natl Acad Sci USA, 2004, 101:

6346–6350

26 Li G, Zhang R, Fan J, Tie X. Impacts of black carbon aerosol on photolysis frequencies and ozone in the Houston area. J Geophys Res, 2005, 110: D23206, doi: 10.1029/2005JD005898

27 Liao H, Adams P J, Chung S H, et al. Interaction between tropospheric chemistry and aerosols in a unified general circulation model. J Geophys Res, 2003, 108: 4001, doi: 10.1029 /2001JD001260

28 Bian H S, Prather M J, Takemura T. Tropospheric aerosol impacts on trace gas budgets through photolysis. J Geophys Res, 2003, 108: 4242, doi: 10.1029/2002JD002743

29 Tang Y H, Carmichael G R, Uno I, et al. Impacts of aerosols and clouds on photolysis frequencies and photochemistry during TRACE-P: 2.Three-dimensional study using a regional chemical transport model. J Geophys Res, 2003, 108(D21): 8822, doi: 10.1029/ 2002JD003100

30 Li Z, Chen H, Cribb M, et al. Preface to special section: Overview of the east asain study of tropospheric aerosols: an international regional experiment (EAST-AIRE). J Geophys Res, 2007, doi: 10.1029/ 2007JD008853

31 Xia X, Chen H, Li Z, et al. Significant reduction of surface solar irradiance induced by aerosols in a suburban region in northeastern China. J Geophys Res, 2007, 112: D22S02, doi: 10.1029/ 2006JD007562

32 Xia X, Li Z, Wang P, et al. Analysis of relationships between ultraviolet radiation (295–385 nm) and aerosols as well as shortwave radiation. Annles Geophys, 2008, 26: 2043–2008

33 Liu J, Xia X, Wang P, et al. Significant aerosol direct radiative effects during a pollution episode in northern China. Geophys Res Lett, 2007, doi: 10.1016/j.atmosenv.2007.05.001

34 Deng X J. The aerosol characterizations and its impacts on visibility and surface ozone in the Pearl River Delta Region (PRD). Doctoral Dissertation. Beijing: Peking University, 2008

35 Wu D, Mao J T, Deng X J, et al. Black carbon aerosols and their radiative properties in the Pearl River Delta region. Sci China Ser D-Earth Sci, 2009, 52: 1150–1163

36 Madronich S, Flocke S. The role of solar radiation in atmospheric chemistry. In: P Boule, ed. Handbook of Environmental Chemistry. Heidelberg: Springer-Verlag, 1999. 1–26

37 Madronich S, Calvert J G. The NCAR Master Mechanism of the Gas Phase Chemistry, Version 2.0, Rep. NCAR/TN~333+STR. Boulder, Colo: Natl Cent For Atmos Res, 1989

38 Madronich S, Calvert J G. Permutation reactions of organic peroxy-radicals in the troposphere. J Geophys Res, 1990, 95: 5697–5715

39 Tyndall G S, Cox R A, Granier C, et al. Atmospheric chemistry of small organic peroxy radicals. J Geophys Res, 2001, 106: 12157–12182

40 Demore W B. Chemical Kinetics and Photochemical Data for Use in Stratospheric Modeling. Pasadena: JPL Publications, 2000

41 Orlando J J, Tyndall G S, Bilde M, et al. Laboratory and theoretical study of the oxy radicals in the OH- and CI- initiated oxidation of ethene. J Phys Chem, 1998, A102: 8116–8123

42 Atkinson R, Baulch D L, Cox R A,et al. Evaluated kinetic and photochemical data for atmospheric chemistry: supplement VIII, halogen species-IUPAC subcommittee on gas kinetic data evaluation for atmospheric chemistry. J Phys Chem Ref Data, 2000, 29: 167–266

43 Christensen L E, Okumura M, Sander S P, et al. Kinetics of HO_2 + HO_2=H_2O_2 + O_2: Implications for stratospheric H_2O_2. Geophys Res Lett, 2002, doi: 10.1029/2001GL014525

44 Sillman S. The use of NO_y, H_2O_2, and HNO_3 as indicators for ozone-NOx-hydrocarbon sensitivity in urban locations. J Geophys Res, 1995, 100: 14175–14188.

45 Wang T, Wu Y Y, Chenug T F, et al. A study of surface ozone and the relation to complex wind flow in Hongkang. Atmos Environ, 2001, 35: 3203–3215

46 National Research Council (NRC). Rethinking the Ozone Problem in Urban and Regional Air Pollution. Committee on Tropospheric Ozone Formation and Measurement. Washington, D.C.: National Academy Press, 1991

47 Colbeck I, Mackenzie A R. Air Pollution by Photochemical Oxidants. Amsterdam: Elsevier, 1994

48 Lam K S, Wang T, Chan L Y, Liu H Y. Observation of surface ozone and carbon monoxide at a coastal site in Hong Kong. Proceedings of the XVIII Quadrennial 1996 Ozone Symposium, 1998, 1: 395–398

49 Chan L Y, Chan C Y. Surface ozone pattern in Hong Kong. J Appl Meteorol, 1998, 37: 1151–1165

50 Luo C, Zhou X J, Lam K S, et al. An nonurban ozone air pollution episode over eastern China: Observation and model simulations. J Geophys Res, 2000, 105: 1889–1908

51 Tonnesen G S, Dennis R L. Analysis of radical propagation efficiency to assess ozone sensitivity to hydrocarbons and NO_x 1.Local indicators of instantaneous odd oxygen production sensitivity. J Geophys Res, 2000, 105: 9213–9225